GEOPHYSICAL RESEARCH LETTERS, VOL. 37, L03502, doi:10.1029/2009GL041872, 2010

Large sea ice outflow into the Nares Strait in 2007

R. Kwok,[1] L. Toudal Pedersen,[2] P. Gudmandsen,[3] and S. S. Pang[1]

Received 20 November 2009; revised 11 December 2009; accepted 11 January 2010; published 9 February 2010.

[1] Sea ice flux through the Nares Strait is most active during the fall and early winter, ceases in mid- to late-winter after the formation of ice arches along the strait, and re-commences after breakup in summer. In 2007, ice arches failed to form. This resulted in the highest outflow of Arctic sea ice in the 13-year record between 1997 and 2009. The 2007 area and volume outflows of 87 × 10^3 km^2 and 254 km^3 are more than twice their 13-year means. This contributes to the recent loss of the thick, multiyear Arctic sea ice and represents ~10% of our estimates of the mean ice export at Fram Strait. Clearly, the ice arches control Arctic sea ice outflow. The duration of unobstructed flow explains more than 84% of the variance in the annual area flux. In our record, seasonal stoppages are always associated with the formation of an arch near the same location in the southern Kane Basin. Additionally, close to half the time another ice arch forms just north of Robeson Channel prior to the formation of the Kane Basin arch. Here, we examine the ice export with satellite-derived thickness data and the timing of the formation of these ice arches. **Citation:** Kwok, R., L. Toudal Pedersen, P. Gudmandsen, and S. S. Pang (2010), Large sea ice outflow into the Nares Strait in 2007, *Geophys. Res. Lett.*, *37*, L03502, doi:10.1029/2009GL041872.

1. Introduction

[2] Arctic Ocean sea ice is exported through Nares Strait, a relatively narrow passage ~30–40 km wide and ~500 km long situated between Greenland and Ellesmere Island (Figure 1). The sea ice cover just north of the strait contains some of the thickest sea ice in the Arctic Basin. Local ice drift is driven by strong northerly winds that are associated with ageostrophic, orographically channeled flow down the atmospheric pressure gradient from the Lincoln Sea to Baffin Bay [*Gudmandsen*, 2000], and the ice drift has been shown to be highly correlated with this along-strait pressure gradient [*Samelson et al.*, 2006]. These prevailing winds drive sea ice out of the Arctic Ocean: this ice volume export represents a negative term in the annual Arctic Ocean mass balance, and the associated meltwater is a source of buoyancy downstream in Baffin Bay with potential impact on deep convection in the Labrador Sea farther south [*Goosse et al.*, 1997].

[3] *Kwok* [2005] examined the seasonal and interannual variability of the Nares Strait outflow using a 6-year record of ice motion from satellite data. Stoppage in ice export is one feature of the seasonal cycle coupled to the formation of persistent sea ice arches along the Strait in the late fall and winter. Arching is a phenomenon quite common in the narrow passages and straits of the Canadian Arctic Archipelago, and an important factor in confining the Arctic ice cover to an enclosed basin [*Hibler et al.*, 2006].

[4] In 2007, no arches were formed. The consequence is a large outflow that contributed to the recent depletion of thick multiyear sea ice [*Kwok et al.*, 2009]. The present note places the 2007 outflow within the context of estimates in area and volume flux, and examines the timing of arch formation over a longer 13-year record between 1997 and 2009. Data sets used include ice drift from RADARSAT and Envisat imagery, and ice thickness is from ICESat.

2. Data Description

2.1. Ice Area Flux and Multiyear Ice Fraction

[5] Ice flux is estimated at a gate positioned at the Lincoln Sea entrance to Nares Strait (Figure 1). The ~30 km wide gate spans the Robeson Channel between Ellesmere Island and Greenland. Ice motion is from tracking the displacement of common ice features in the wide-swath RADARSAT and Envisat SAR imagery (resolution: ~150 m) using an image-matching scheme described by *Kwok et al.* [1990]. Between 1996 and 2007, only RADARSAT coverage of the Nares Strait region was available. The temporal sampling is nominally 3 days although a small fraction of motion estimates were over a longer period. After April 2007, Envisat provided near-daily coverage of the flux gate. The *n*-day ice motion is sampled on a 5-km grid that covers an area of ~30 km to the north and south of the gate. All motion vectors are visually inspected for quality and corrected or replaced where needed.

[6] Area flux is computed by interpolating the gridded ice motion (5 km grid) to the gate and integrating the gate-perpendicular component of the motion profile along the gate. Due to gradients in ice motion, flux estimates using grid measurements in proximity of the gate (i.e., within 5 km) have lower uncertainty. The expected uncertainty in the displacements is ~300 m. Assuming errors of the motion samples to be additive, unbiased, uncorrelated and normally distributed, the uncertainties in the area flux over any given time interval, σ_F, can be computed viz. [*Kwok,* 2009]: $\sigma_F = \sigma_u L/\sqrt{N_s}$. L is the width of the flux gate, σ_u is the standard error in the displacement estimates, and N_s is the number of independent samples. For $N_s = 6$ (number of 5 km samples along the 30 km gate) and $\sigma_u = 300$ m, the uncertainty in area flux is ~4 km^2 over the sampling interval.

[7] The coverage of the two primary ice types (first-year and multiyear ice) at the gate is derived from the SAR imagery using a backscatter-based procedure [*Kwok et al.*, 1992] that exploits the large contrast in scattering cross-

[1]Jet Propulsion Laboratory, California Institute of Technology, Pasadena, California, USA.
[2]Danish Meteorological Institute, Copenhagen, Denmark.
[3]Danish National Space Center, Technical University of Denmark, Lynby, Denmark.

0094-8276/10/2009GL041872$05.00

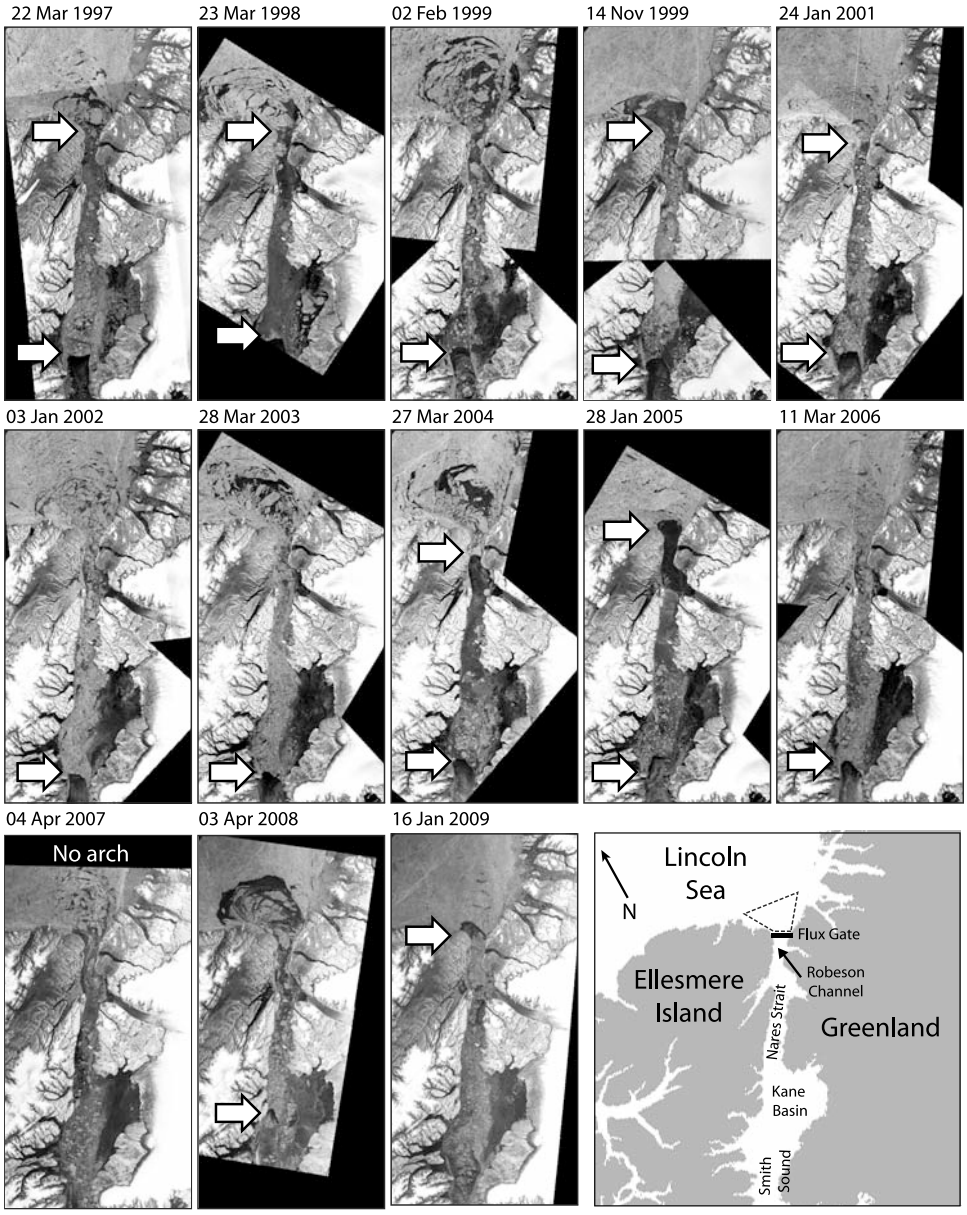

Figure 1. Nares Strait flux gate and ice arches. The flux gate, at the entrance to Robeson Channel, spans a width of ~30 km between Ellesmere Island and Greenland. Synthetic aperture radar (SAR) imagery shows the location of the ice arches, following the cessation of ice export, at the entrance to Robeson Channel and southern Kane Basin for the 13 years between 1997 and 2009. White arrows show the location of the arches after they were formed. Ice thickness used in the flux estimates is the average of the ICESat samples inside the dashed polygon. (RADARSAT imagery ©CSA 2009, Envisat imagery ©ESA 2009).

section between the two ice types. Each SAR image pixel is classified as a member of one of these two types. Broad assessments of the quality of these estimates are given by *Kwok and Cunningham* [2002] and have been shown to be relatively robust during the winter. During the melt season (July–September), when the above procedure does not allow effective discrimination of the ice types we take the multiyear ice fraction to be that estimate we obtain at the end of June.

2.2. Ice Volume Flux Estimates

[8] Ice thickness is from the gridded fields of the ten ICESat campaigns (two per year: one in the fall and the other in winter) between 2003 and 2008 [*Kwok et al.*, 2009]. Each fall and winter ICESat campaign covers a ~33-day period between mid-October and mid-November (2003–2007), and between late February and late March (2004–2008). We use the spatial average of the thickness within a polygon (in the Lincoln Sea just north of the flux gate; see Figure 1) as the thickness of the multiyear (MY) sea ice entering the strait. Since there are only two ICESat thickness estimates each year, we take the average thickness of the two campaigns to be the annual mean MY thickness. To account for the volume of the seasonal ice, we assume the thickness of the first-year (FY) ice to be 1.5 m as most of the seasonal ice are created by deformation of the thick pack

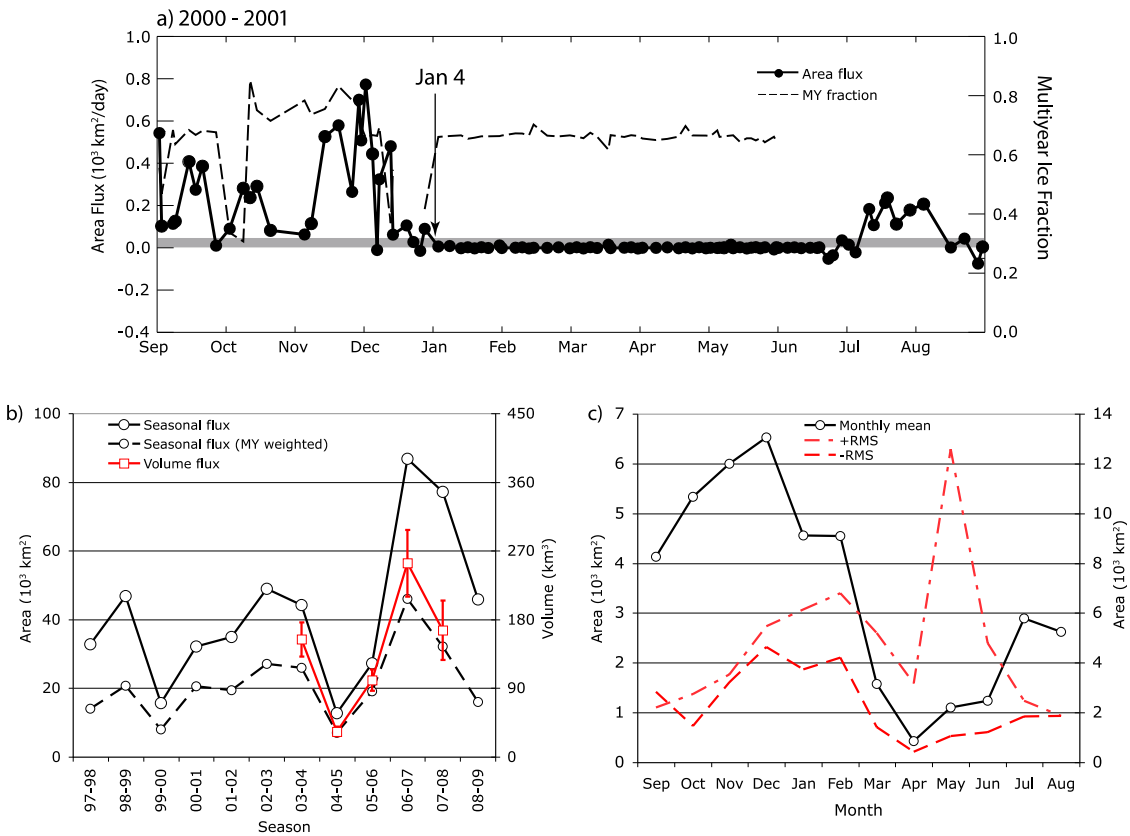

Figure 2. Annual (September through August) outflow of sea ice area and volume through the Nares Strait flux gate (1997–2009). (a) Time series of daily ice area flux and multiyear ice fraction between September 2000 and August 2001. Gray band shows the threshold of 50 km^2/day used in the determination of stoppage. (b) Total area flux (black line), multiyear year ice area flux (dashed line), and volume flux (red line). (c) Mean and variance (+rms, −rms) of monthly outflow over the same period. The scale of the red dashed lines is on the right side of the plot.

just north of the flux gate (see Figure 1) and are relatively young when exported with the thick ice. The total annual volume flux is then the weighted sum of the product of the annual ice area flux, and the annual mean ice thickness of the MY and FY ice. Uncertainty in the ICESat thickness estimates is ~0.5 m.

3. Ice Flux: Area and Volume Record (1997–2009)

[9] Figure 2a shows a sample record of Nares Strait flux between September 2000 and August 2001. The most striking feature in this particular annual record is the complete stoppage in January, which then re-commences after breakup in early July. This cessation of ice drift can be attributed to the formation of ice arches along the strait. These arches serve to block the movement and export of Arctic sea ice. Depending on the year, ice arches form typically at one or both of the following two locations (discussed later): one at the entrance to Robeson Channel and the other at Kane Basin near the southern end of Nares Strait (see Figure 1).

[10] The 13-year record (1997 through 2009) of total and MY ice area flux is shown in Figure 2b. The mean annual (September–August) ice area flux is 42 × 10^3 km^2 with a standard deviation of 22 × 10^3 km^2. This can be compared to the estimate of 33 × 10^3 km^2 for the 6-year record between 1997 and 2002 [*Kwok*, 2005]. The flux of MY ice area, as expected, is lower. Over this longer 13-year record, the total area flux ranges from a low of 13 × 10^3 km^2 in 2004 to a high of 87 × 10^3 km^2 in 2007. In 2007, no arches were formed and the unobstructed ice outflow at Nares Strait was the highest on record: this area flux was more than twice the annual mean. This was followed by the second highest year in 2008. The monthly variability in area is high (Figure 2c). On average, there seems to be a seasonal cycle with the highest ice flux between September and February, which decreases quite rapidly in early spring and through summer. The large variability (+rms) in May, a month of typically low average ice flux, is due to the anomalously high ice flux in May of 2007.

[11] Because of the on-off nature of ice flux associated with the formation of the ice arches, it is interesting to examine the dependence of ice flux on the prolonged periods of near-zero flux within each annual cycle. We define the length of each period (T_z) as the number of consecutive days with ice flux <50 km^2. Using this criterion, the average length of near-zero outflow is ~184 days (~6 months) and ranges between zero in 2007 and 233 days in 1998. Correlation of the area outflow and the days of active outflow (i.e., $T_a = 365 - T_z$) shows that T_a explains ~82% of the variance in annual ice flux. Figure 3 shows the correspondence between the annual area flux and T_a over the

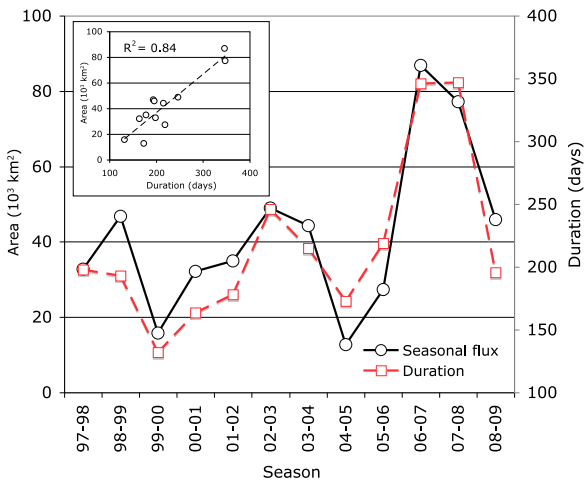

Figure 3. Annual (September through August) ice area flux and duration of continuous sea ice outflow. Scatterplot (inset) shows the correlation of the ice area outflow and duration of outflow.

13-year record and the remarkable correlation is shown in the inset. Clearly, these ice arches are key in the control of the outflow of Arctic Ocean sea ice through the Nares Strait. This is the case in spite of the large and variable drift speeds that are dependent on local winds and currents, and coastal geometry. Surface winds along the Nares Strait tend to be channeled by orographic features reaching 500–2000 m on both sides of the passage; and, strong drainage and katabatic winds from nearby outlet glaciers contribute to the variability in local surface wind forcing [*Samelson and Barbour*, 2008].

[12] Of greater geophysical interest is the contribution this ice flux on the depletion of the mass/volume of the Arctic Ocean ice cover. Using the methodology described earlier, the volume flux estimates for the five years using ICESat thickness data is shown in Figure 2b. The average thickness (fall and winter average) of the sea ice just north of the strait is relatively thick at 4.7, 5.4, 5.5, 4.8, and 4.3 m for the 5-year ICESat record. Compared to the basin-wide winter average thickness of ~2.9 m [*Kwok et al.*, 2009], this area contains some of the thickest sea ice in the Arctic Ocean. The error bars (in red) reflect the uncertainties in volume estimates associated with the 0.5 m errors in thickness. The 5-year average volume flux is 141 km^3 with a low of 33 km^3 in 2004 and a high of 254 km^3 in 2007. The average flux can be compared to the rough estimate of 130 km^3 by *Kwok* [2005]. In the absence of ice arches in 2007, the large ice volume exported represents ~10% of the mean ice export at Fram Strait [*Kwok*, 2009].

4. Timing of the Formation of Nares Strait Ice Arches

[13] Arching (the formation of arches) is typical at two locations along the Nares Strait (Figure 1). In addition to the arch at the entrance to Robeson Channel, noted by *Kwok* [2005], there is another found at Kane Basin to the south end of Nares Strait (discussed by *Barber et al.* [2001]). They are separated by ~450 km. Visual inspection of the 13 years of SAR imagery indicates that these are the two predominant arches that control the ice motion in the strait and thus the flux of ice from the Arctic. Henceforth, we refer to them as the N arch (North) and S arch (South), respectively. Arching also occurs occasionally at other locations along the strait, but they rarely persist for long periods (1–2 months) of time. For example, an ice arch formed at the entrance to Kennedy Channel in June of 2005 stopping the ice drift for ~3 weeks.

[14] Once these quasi-static arches are formed, their structural strengths are able to withstand ice pressures, associated wind and ocean forcing, for prolonged periods in the winter and spring. In addition, they may be strengthened, once formed, by thermodynamic processes (ice growth), so that their breaking strength increases with time. Multibeam sonar mapping from an icebreaker suggests that ice scouring in the vicinity of the S arch from very thick multiyear and or icebergs may ground in this region, thereby slowing down the flux of ice, in concert with other conditions, for a period sufficient for thermodynamic growth to solidify the arch (D. G. Barber, personal communication, 2009). As arching of the sea ice in the Nares Strait controls Arctic ice export, we examine here the timing of their formation and the interannual variability of this timing. This will be useful for elucidating the physical mechanisms involved in arching, and provide an indication of their potential variability in a changing climate and the consequences of their absence.

[15] Table 1 shows the approximate date of formation of the two arches, the delay in the formation of the S arch relative to the N arch, and the duration of ice flux stoppage at our flux gate at the entrance to the Strait. We determine the date of formation of the N arch as that date where an obstruction in the shape of an arch forms (by visual inspection of the SAR imagery) and when the ice discharge from the Arctic goes to zero (using ice drift). Typically, there is higher backscatter thick multiyear ice to the north of the arch and lower backscatter seasonal ice or a mixture of ice types to the south after stoppage (e.g., March 2004 and January 2005 in Figure 1), but the cessation of ice drift provides the best indication as the arch is sometimes not visible because of the mixture of ice in the channel and the limited spatial resolution of the data. The dating of the formation of the S arch is more straightforward as there is almost always easily identifiable open water south of the

Table 1. Approximate Dates of Formation of the N and S Arches[a]

Season	N Arch (Date)	S Arch (Date)	Delay (Days)	Stoppage (Days)
96–97	5-Mar-97 ± 4	15-Mar-97 ± 5	10	224
97–98	5-Feb-98 ± 2	13-Mar-98 ± 2	36	215
98–99		24-Jan-99 ± 5		214
99–00	29-Oct-99 ± 2	13-Nov-99 ± 2	15	281
00–01	4-Jan-01 ± 3	14-Jan-01 ± 3	10	256
01–02		10-Dec-02 ± 3		214
02–03		23-Feb-03 ± 6		166
03–04	14-Feb-04 ± 1	11-Mar-04 ± 7	26	158
04–05	7-Dec-04 ± 1	31-Dec-04 ± 1	24	242
05–06		18-Feb-06 ± 3		169
06–07				
07–08		1-Apr-08 ± 1		68
08–09	16-Jan-09 ± 1			174
Avg	12-Jan ± 44	2-Feb ± 44	20 ± 10	184 ± 10

[a]For the seasons where there are two arches, the north one forms before the south (delay in days). The duration of stoppage is determined using ice flux (see discussion in text).

structure (i.e., the North Water Polynya). The uncertainty in the timing estimates associated with the interval between image coverage is indicated in Table 1. A blank entry indicates that there was no arching during that season.

[16] Arching typically occurs between late fall and mid-winter (Table 1). Average dates of formation of the N and S arches are 12 January (±44 days) and 2 February (±44 days). This establishes a clear seasonal preference for arch formation. Disintegration occurs on average 184 ± 10 days after flux stoppage. Since no ice arch has been observed to survive for longer than a season, thermodynamics seems to determine the limits of their survivability under current climate conditions. Melt and warmer ice temperatures reduce the cohesive strength of the arches through the summer, particularly in the presence of northerly winds that tend to break-up the ice edge [*Barber et al.,* 2001].

[17] In our 13-year record, when both arches are present, the S arch is always formed after the formation of the N arch: the average lag is ~20 ± 10 days. The S arch was absent only in 2009 and the N arch was solely responsible for the flux stoppage. In contrast, the N arch was present in just less than half of the record. And, in 2007 no arches were formed. The temporal proximity of their formation suggests that the S arch may be coupled to the arching in the north. When the N arch forms, the fraction and compactness of the multi-year ice just south of the arch is reduced as the thick ice within the strait is discharged into Baffin Bay. But, the question of whether the arching in southern Kane Basin is dependent on the upstream ice conditions, ocean tides, local bathymetry, and/or coastal conditions remains. However, it is clear that with years when only the S arch is present, there exist conditions where this arch could form without the formation of the ice arch at the entrance to Nares Strait. During the winter of 2007, none of the mitigating conditions for arching were met and no arches were formed.

[18] Field observations by one of us (*PG*) indicate that these ice arches seem to be a mélange of MY ice floes 'glued' together with younger ice, consistent with the behavior of a granular material flowing through chutes and funnels [*Sodhi*, 1977]. But because of the small spatial length scales involved, it is problematic to use large-scale fields (e.g., NCEP/NCAR) to attempt to characterize the locally complex meteorological [*Samelson and Barbour*, 2008] and ocean [*Münchow and Melling*, 2008] conditions associated with arching. In situ observations from field programs are vital for detailed understanding of the local conditions favorable to arch formation.

5. Conclusions

[19] In the present note, we examined 13 years (1997–2009) of Arctic Ocean sea ice export through the Nares Strait and highlighted the large outflow in 2007. Ice drift and estimates of multiyear sea ice coverage are from high-resolution SAR imagery acquired by RADARSAT and Envisat, and ice thickness is from ICESat. We estimate an average annual (September–August) ice area flux of 42 × 10^3 km^2 and an average annual volume flux of 141 km^3. This can be compared to the annual average area and volume flux of 33 × 10^3 km^2 and ~130 km^3 from a shorter 6-year record between 1996 and 2002 [*Kwok*, 2005]. The larger averages in the longer record are due to two consecutive years (2007 and 2008) of high outflows.

[20] Seasonal stoppages of Arctic outflow are controlled by the formation of two predominant ice arches: one located at the entrance to Robeson Channel and the other in southern Kane Basin. These arches did not form in 2007 and the duration of stoppage was shortest in 2008 resulting in the two highest outflows on record. These two years (2007/2008) have contributed to the depletion of the area (87/77 × 10^3 km^2) and volume (254/166 km^3) of the thick multiyear sea cover of the Arctic. The ice volume exported in 2007 represents >10% of the mean ice export at Fram Strait [*Kwok*, 2009]. Compared to the basin-scale winter average thickness of ~2.9 m [*Kwok et al.*, 2009] we note that the exported ice (at 4–5 m) found north of Nares Strait represent some of the thickest ice in the Arctic Ocean. This thick, old ice occupies the tails of the thickness distribution and takes years with the right conditions to replenish.

[21] If there is a decreased likelihood of arch formation as the ice cover becomes thinner and weaker due to warming, there is the potential for the Nares Strait to shift to a higher flow state. In the face of a rapidly declining MY sea ice cover [*Kwok et al.*, 2009], the outflow at Nares Strait could contribute significantly to the depletion of the multiyear sea ice area and volume of the Arctic Ocean, and thus the decline in summer ice coverage. Separately, increased flux of ice into the North Water Polynya could dramatically alter its overall productivity thus significantly changing the primary, secondary and high trophic ecosystem use of this polynya [*Barber and Massom*, 2007].

[22] **Acknowledgments.** We are grateful to CSA and ESA for providing the SAR imagery used in this analysis. This work was performed at the Jet Propulsion Laboratory, California Institute of Technology, and is sponsored by the National Science Foundation and the National Aeronautics and Space Administration.

References

Barber, D. G., and R. A. Massom (2007), The role of sea ice in Arctic and Antarctic polynyas, in *Polynyas: Windows to the World*, edited by W. O. Smith and D. G. Barber, *Elsevier Oceanogr. Ser.*, *74*, 1–54.

Barber, D., R. Marsden, P. Minnett, G. Ingram, and L. Fortier (2001), Physical processes within the North Water (NOW) Polynya, *Atmos. Ocean*, *39*, 163–166.

Goosse, H., T. Fichefet, and J.-M. Campin (1997), The effects of the water flow through the Canadian archipelago in a global ice ocean model, *Geophys. Res. Lett.*, *24*, 1507–1510, doi:10.1029/97GL01352.

Gudmandsen, P. (2000), A remote sensing study of Lincoln Sea, paper presented at ERS-ENVISAT Symposium, Eur. Space Agency, Gothenburg, Sweden.

Hibler, W. D., III, J. K. Hutchings, and C. F. Ip (2006), Sea ice arching and multiple flow states of Arctic pack ice, *Ann. Glaciol.*, *44*, 339–344, doi:10.3189/172756406781811448.

Kwok, R. (2005), Variability of Nares Strait ice flux, *Geophys. Res. Lett.*, *32*, L24502, doi:10.1029/2005GL024768.

Kwok, R. (2009), Outflow of Arctic sea ice into the Greenland and Barents Seas: 1979–2007, *J. Clim.*, *22*, 2438–2457, doi:10.1175/2008JCLI2819.1.

Kwok, R., and G. F. Cunningham (2002), Seasonal ice area and volume production of the Arctic Ocean: November 1996 through April 1997, *J. Geophys. Res.*, *107*(C10), 8038, doi:10.1029/2000JC000469.

Kwok, R., J. C. Curlander, R. McConnell, and S. Pang (1990), An ice motion tracking system at the Alaska SAR Facility, *IEEE J. Oceanic Eng.*, *15*, 44–54, doi:10.1109/48.46835.

Kwok, R., E. Rignot, B. Holt, and R. G. Onstott (1992), Identification of sea ice type in spaceborne SAR data, *J. Geophys. Res.*, *97*, 2391–2402, doi:10.1029/91JC02652.

Kwok, R., M. Wensnahan, I. Rigor, H. J. Zwally, and D. Yi (2009), Thinning and volume loss of Arctic sea ice: 2003–2008, *J. Geophys. Res.*, *114*, C07005, doi:10.1029/2009JC005312.

Münchow, A., and H. Melling (2008), Ocean current observations from Nares Strait in the west of Greenland: Interannual to tidal variability and forcing, *J. Mar. Res.*, *66*, 801–833.

Samelson, R., and P. L. Barbour (2008), Low-level jets, orographic effects, and extreme events in Nares Strait: A model-based mesoscale climatology, *Mon. Weather Rev.*, *136*, 4746–4759, doi:10.1175/2007MWR2326.1.

Samelson, R. M., T. Agnew, H. Melling, and A. Munchow (2006), Evidence for atmospheric control of sea-ice motion through Nares Strait, *Geophys. Res. Lett.*, *33*, L02506, doi:10.1029/2005GL025016.

Sodhi, D. S. (1977), Ice arching and the drift of pack ice through restricted channels, *Rep. 77-18*, Cold Reg. Res. and Eng. Lab., Hanover, N. H.

P. Gudmandsen, Danish National Space Center, Technical University of Denmark, DK-2800 Lynby, Denmark.

R. Kwok and S. S. Pang, Jet Propulsion Laboratory, California Institute of Technology, Pasadena, CA 91109, USA. (ron.kwok@jpl.nasa.gov)

L. Toudal Pedersen, Danish Meteorological Institute, DK-2100 Copenhagen, Denmark.